Received: 6 February 2018 | Revised: 23 July 2019 | Accepted: 3 August 2019

DOI: 10.1002/nbm.4171

RESEARCH ARTICLE

WILEY NMR IN BIOMEDICINE

Improved off-resonance phase behavior using a phase-inverted adiabatic half-passage pulse for ^{13}C MRS in humans at 7 T

Eulalia Serés Roig[1] | Lijing Xin[2] | Daniel Gallichan[2] | Vladimir Mlynarik[3] | Rolf Gruetter[1,2,4,5]

[1] Laboratory of Functional and Metabolic Imaging (LIFMET), Ecole Polytechnique Fédérale de Lausanne (EPFL), Switzerland

[2] Centre d'Imagerie Biomédicale—Animal and Imaging Technology (CIBM-AIT), Lausanne, Switzerland

[3] High Field MR Center, Department of Biomedical Imaging and Image-Guided Therapy, Medical University of Vienna, Vienna, Austria

[4] Department of Radiology, University of Lausanne (UNIL), Switzerland

[5] Department of Radiology, University of Geneva (UNIGE), Switzerland

Correspondence
Eulalia Serés Roig, Ecole Polytechnique Fédérale de Lausanne (EPFL), EPFL-SB-IPSB-LIFMET, Station 6, CH-1015 Lausanne. Switzerland.
Email: eulalia.seresroig@epfl.ch

Present Address
Daniel Gallichan, Cardiff University Brain Research Imaging Centre, Cardiff, UK

Funding information
Leenaards and Jeantet Foundations; Ecole Polytechnique Fédérale de Lausanne (EPFL); Centre Hospitalier Universitaire Vaudois (CHUV); Hôpitaux Universitaires de Genève (HUG); Université de Genève (UNIGE); Centre d'Imagerie Biomédicale (CIBM)

In vivo ^{13}C MRS at high field benefits from an improved SNR and spectral resolution especially when using surface coils in combination with adiabatic pulses, such as the adiabatic half-passage (AHP) pulse for ^{13}C excitation. However, the excitation profile of the AHP pulse is asymmetric relative to the carrier frequency, which could lead to asymmetric excitation of the spectral lines relative to the center of the spectrum. In this study, a pulse-acquire sequence was designed for adiabatic ^{13}C excitation with a symmetric bandwidth, utilizing a combination of two AHP pulses with inverted phases in alternate scans.

Magnetization and phase behavior as a function of frequency offset and RF amplitude of the B_1 field, as well as the steady-state transverse magnetization response to off-resonance, were simulated. Excitation properties of the combined pulse sequence were studied by ^{23}Na imaging and ^{13}C spectroscopy in vitro on a phantom and in vivo on the human calf at 7 T.

Simulations demonstrated symmetric transverse magnetization and phase with respect to positive and negative frequency offsets when using two AHP pulses with inverted phases in alternate scans, thereby minimizing baseline distortion and achieving symmetric T_1 weighting, as confirmed by in vitro measurements. The intensities of the lipid peaks at 15, 30, 62, 73, and 130 ppm were in agreement with those theoretically predicted using two AHP pulses with inverted phases in alternate scans.

We conclude that using two phase-inverted AHP pulses improves the symmetry of the ^{13}C excitation profile and phase response to off-resonance effects at 7 T in comparison with using a single AHP pulse.

KEYWORDS

^{13}C excitation bandwidth, ^{13}C nucleus, adiabatic half-passage (AHP), human calf at 7 T, natural abundance ^{13}C resonances, off-resonance

Abbreviations: ^{13}C, carbon-13; ^{1}H, hydrogen-1; ^{23}Na, sodium-23; 2D, two dimensional; ^{31}P, phosphorus-31; 3D, three dimensional; AHP, adiabatic half-passage; BIR-4, B_1-insensitive rotation with four segments; FLASH, fast low-angle shot; FOV, field of view; HS, hyperbolic secant; IAHP, phase-inverted adiabatic half-passage; M_{xy}, transverse magnetization; M_z, longitudinal magnetization; NaCl, sodium chloride; ppm, parts per million; SAR, specific absorption rate; SNR, signal-to-noise ratio; T_I, inversion time.; T_R, repetition time

1 | INTRODUCTION

Carbon-13 magnetic resonance spectroscopy (^{13}C MRS) benefits from an improved signal-to-noise ratio (SNR) and spectral resolution at ultra-high field (i.e. 7 T and above). Largely as a result of the wide ^{13}C chemical shift range,[1] unique insights into carbohydrate metabolism in vivo are possible.[2] Due to the low sensitivity of the natural abundance ^{13}C isotope, in vivo ^{13}C MRS is commonly performed using surface coils, as the high filling factor provided by surface coils results in increased SNR,[3] while the B_1 inhomogeneities these surface coils incur can be mitigated using adiabatic RF excitation.[4-8]

A common adiabatic RF pulse employed for single-resonance excitation is the adiabatic half-passage (AHP) pulse, derived from the classical adiabatic full-passage pulse.[4,9,10] The main feature of the AHP pulse is the ability to achieve uniform 90° excitation of the magnetization despite the B_1 inhomogeneities present. However, this is only strictly valid on-resonance as the excitation bandwidth of the AHP pulse is asymmetric,[5] leading to asymmetric excitation of the spectral lines relative to the center of the spectrum. In addition, the inherent offset-dependent phase variations of the AHP pulse may cause phase distortion of spectral lines and baseline distortion, which may affect the accuracy of spectral quantification.

An alternative to minimize the inherent offset phase variations of the AHP pulse is to invert the effective field during the pulse in alternate scans. This allows opposite single rotations resulting in a symmetric excitation that minimizes phase distortions. This method was first introduced for rapid estimation of saturation factors for in vivo surface coil phosphorus-31 (^{31}P) MRS in the human calf muscle at 2.35 T.[11] Another alternative is the well-known adiabatic BIR-4 (B_1-insensitive rotation with four segments) pulse,[12] which further improves the inherent offset effects of the AHP pulse, as it has the additional ability to achieve plane rotations within a symmetric excitation bandwidth, as first demonstrated for ^{31}P MRS using phantom samples at 4.7 T.[12] More recently, the above mentioned method using two AHP pulses with inverted effective fields in alternate scans[11] has been extended to higher field for in vivo ^{31}P MRS cardiac and calf muscle in humans at 3 T,[13] where the scheme was compared with the BIR-4 pulse and was demonstrated to be advantageous in terms of RF power requirements at 3 T. This was explained as due to the higher RF power requirements of the BIR-4 pulse at 3 T than at 1.5 T for a given pulse duration, while the scheme using frequency sweep cycles could use a short pulse duration to alleviate T_2 relaxation effects without increasing the RF power. So far, however, the effect on phase distortion by these adiabatic pulses[11-13] has not been demonstrated for ^{13}C MRS at high field. Therefore, the aim of this present study was to achieve symmetric adiabatic excitation for in vivo ^{13}C MRS in human muscle at 7 T using two single AHP pulses with inverted phases applied in alternate scans.

2 | METHODS

All experiments were performed on a 7 T human MR scanner (Siemens Erlangen/Germany). For these measurements, a ^{13}C-^{1}H RF surface coil was built, consisting of a combination of a linear-^{13}C coil and a quadrature-^{1}H coil[14] tuned for 7 T. Informed consent was obtained from all subjects according to the procedure approved by the local ethics committee.

2.1 | Pulse sequence implementation

Four pulse-acquire sequences with AHP for ^{13}C excitation were implemented: (1) using an AHP pulse, (2) using a phase-inverted AHP (IAHP), (3) combining an AHP and an IAHP pulse in alternate scans (AHP + IAHP), and (4) using a B_1-insensitive BIR-4 pulse.[12] The WALTZ-16 scheme[15] was used to achieve broadband ^{1}H decoupling during ^{13}C signal acquisition.

2.2 | Bloch simulations

To evaluate and compare the AHP, IAHP, and AHP + IAHP pulses in terms of offset dependence of magnetization and phase, a Bloch simulator was developed and implemented in MATLAB (MathWorks, Natick, MA, USA). In addition, the offset magnetization and phase of the AHP + IAHP pulse was compared with the B_1-insensitive BIR-4 pulse[12] with an identical AHP segment.

Simulations were performed using an AHP pulse characterized by the hyperbolic tangent/tangent (tanh/tan) amplitude/frequency ($B_1(t)/f(t)$) modulation (number of points = 254). The length of the AHP pulse was fixed and chosen equal to that used for the in vitro and in vivo measurements (2050 μs). Consequently, because of the short RF pulse length relative to the relaxation times of carbons in the studied metabolites, T_1 and T_2 relaxations were neglected in the Bloch simulations. The IAHP pulse was simulated as identical to the AHP pulse, but with the phase elements conjugated.

To evaluate and compare the performance of the sequences (AHP, IAHP, AHP + IAHP, and BIR-4) in response to off-resonance conditions, three sets of simulations were performed.

First, to determine the RF amplitude ($\gamma B_1/2\pi$) required for AHP to achieve 90° flip angle on-resonance (adiabaticity threshold), both transverse (M_{xy}) and longitudinal (M_z) magnetizations were simulated for a range of RF amplitudes ($\gamma B_1/2\pi$). Second, the transverse magnetization (M_{xy}),

longitudinal magnetization (M_z), and phase of the transverse magnetization were simulated for a fixed RF amplitude ($\gamma B_1/2\pi$ = 2 kHz) above the adiabaticity condition. Third, simulations were extended to test over a range of RF amplitudes ($\gamma B_1/2\pi$).

2.3 | In vitro ^{23}Na MRI

To evaluate the performance of the sequence, in vitro ^{23}Na MRI images were acquired on a phantom containing 100 mM of sodium chloride (NaCl) in solution with DPBS (Dulbecco's phosphate-buffered saline).

Due to the low sensitivity of the ^{13}C signal, MRI experiments were performed using the sodium ^{23}Na nucleus rather than the ^{13}C nucleus, because the ^{23}Na frequency at 7 T (79 MHz) is very close to the ^{13}C frequency at 7 T (75 MHz), while the signal intensity from ^{23}Na is much higher, which allows imaging experiments to be performed more easily. Therefore, for this measurement the linear ^{13}C coil was temporarily retuned to the ^{23}Na resonance frequency (79 MHz at 7 T). The ^{23}Na images were acquired using the two-dimensional (2D) fast low-angle shot (FLASH) sequence, adapted for ^{23}Na nuclei and adiabatic excitation. The transmit voltage required to achieve a 90° flip angle on-resonance was calibrated by testing over a range of transmit voltages (5 V to 50 V in 5 V steps, from 50 V to 100 V in 10 V steps, and from 100 V to 160 V in 20 V steps), and the voltage needed to achieve the adiabatic condition was selected. B_0 shimming was performed using the Siemens three-dimensional (3D) shim routine. The ^{23}Na 2D images were acquired on- and off-resonance (±1 kHz) and both magnitude and phase using AHP, IAHP, AHP + IAHP, and BIR-4 were depicted and compared. The MR protocol was as follows: FLASH 2D sequence using AHP, IAHP, and BIR-4 pulse for excitation (2050 μs), T_R = 300 ms, T_E = 3.7 ms, field of view (FOV) = 128 × 128 mm^2, matrix 64 × 64, spatial resolution = 2 × 2 mm^2, bandwidth = 260 Hz, 5 averages.

2.4 | In vitro ^{13}C MRS

To validate Bloch simulations with in vitro ^{13}C MRS experiments, measurements were made using two phantoms.

First, a small sphere (7 mm diameter) containing 99% ^{13}C-enriched formic acid was placed in the center of the ^{13}C-coil, in which the B_1 field is considered homogeneous. The bandwidth of each sequence (AHP, IAHP, AHP + IAHP, and BIR-4) was measured by exciting formic acid at frequency offsets in a range of ±1 kHz in 50 Hz steps. The following MR parameters were used: T_R = 10 s, vector size 2048, bandwidth 20 kHz, decoupling duration 87 ms, 2 averages. For comparing measured and simulated bandwidth, the measured bandwidth provided by each pulse sequence was normalized to unity (spectra within the measured bandwidth were divided by the maximum signal intensity on-resonance) and superimposed on the corresponding simulated transverse magnetization (M_{xy}) at the given $\gamma B_1/2\pi$ for the AHP pulse.

Second, to investigate the T_1 weighting effects during multiple averaging, a phantom containing 8 mM of 99% ^{13}C-1 labeled glucose solution was used. In order to choose an adequate repetition time ($T_R \leq T_1$), the ^{13}C longitudinal relaxation time T_1 of glucose β was measured by the inversion recovery method, using a hyperbolic secant (HS) pulse for inversion and an AHP pulse for excitation. The voltage required for the HS pulse was set to invert glucose β on-resonance in the sensitive volume of the ^{13}C surface coil. The glucose β peaks on-resonance were measured using the inversion times (T_I) 0.0001, 0.1, 0.5, 1, 2, 4, and 8 s, while T_R = 8 s was used, well above the estimated T_1 value. The experimental glucose β signal intensities were fitted using a single exponential decay in MATLAB: $f(t) = a[1 - b\exp(-T_I/T_1)]$, to calculate the T_1 of glucose β. The glucose β ^{13}C signal was then measured on- and off-resonance (±1 kHz), using the AHP, IAHP, AHP + IAHP, and BIR-4 sequences with the following parameters: T_R = 1 s, vector size = 2048, bandwidth = 20 kHz, decoupling duration = 87 ms, 64 averages.

In addition, the measured glucose β ^{13}C signals were compared with the simulated averaged steady-state transverse magnetization (M_{xy}) off-resonance (±1 kHz), for each sequence. Simulations were performed following 10 excitations using AHP, IAHP, AHP + IAHP, and BIR-4, and because of the short pulse length (2 ms) no signal loss was expected due to relaxation during the pulse. Therefore, T_1 and T_2 relaxation times were only included between excitations rather than during the pulse, T_1 = 1.5 s, T_2 = 0.2 s and T_R = 1 s.

2.5 | In vivo ^{13}C MRS

To investigate the feasibility of the scheme in vivo, non-localized ^{13}C MRS measurements were made on the human calf of a healthy male volunteer. In particular, muscle rather than brain measurements were made because brain measurements would require infusion of ^{13}C substrates due to the low concentration of ^{13}C natural abundance brain metabolites, while natural abundance of ^{13}C glycogen in muscle is high enough to be measured without infusion.

A small sphere containing 99% ^{13}C-enriched formic acid was placed at the center of the ^{13}C coil to be used as an external reference.16,17 The in vivo protocol for ^{13}C MRS included a pulse-acquire sequence with an AHP, IAHP, AHP + IAHP, and BIR-4 pulse for ^{13}C excitation (2050 μs) (the carrier frequency of the pulse was set on the glycogen C_1 peak), together with WALTZ-16 ^{1}H-decoupling (20 ms) during acquisition (T_R = 1.2 s, 256 averages, vector size 2048, acquisition time 102 ms, bandwidth 20 kHz). Shims were adjusted using the first and second order FAST(EST) MAP.[18] Intensities of the ^{13}C peaks obtained using the AHP + IAHP sequence were compared with those obtained using the AHP, IAHP, and BIR-4 pulses.

2.6 | In vivo ^{23}Na MRI

To validate the performance of the sequence with in vivo ^{23}Na MRI, imaging measurements were made on the calf of the same volunteer as above.

The in vivo protocol for ^{23}Na MRI included a 2D FLASH sequence, adapted for ^{23}Na nuclei and adiabatic excitation. The transmit voltage required to achieve a 90° flip angle on-resonance was calibrated by testing over a range of transmit voltages (from 5 V to 20 V in 5 V steps, and from 20 V to 120 V in 20 V steps), and the voltage needed to achieve the adiabatic condition was selected. The ^{23}Na 2D images were acquired on- and off-resonance (±1 kHz) and both magnitude and phase using AHP, IAHP, AHP + IAHP, and BIR-4 were depicted and compared. The MR protocol was as follows: FLASH 2D sequence using AHP, IAHP, and BIR-4 pulse for excitation (2050 μs), T_R = 300 ms, T_E = 3.7 ms, FOV = 128 × 128 mm^2, matrix 64 × 64, spatial resolution = 2 × 2 mm^2, bandwidth = 260 Hz, 5 averages.

3 | RESULTS

3.1 | Bloch simulations

The adiabaticity condition of the AHP pulse on-resonance was achieved at a peak B_1 of 650 Hz. Thus, the following simulations were performed with a peak RF amplitude of 2 kHz, well above the adiabaticity threshold.

The offset dependence of magnetization and phase produced by the IAHP sequence was a mirror image of that produced by the AHP sequence (Figure 1A-H), while the AHP + IAHP sequence characteristics were symmetric relative to the center frequency of the pulses (Figure 1I-L). The simulated longitudinal magnetization (M_z) produced by AHP (Figure 1B) and IAHP (Figure 1F) show that full excitation (M_z = 0) was achieved only on-resonance, whereas full or nearly full ($M_z \approx 0$) excitation for AHP + IAHP (Figure 1J) was achieved over a broader off-resonance range (±1 kHz). Similarly, the phase of the transverse magnetization produced by AHP (Figure 1C and 1D) and IAHP pulses (Figure 1G and 1H) was zero only on-resonance, whereas for the AHP + IAHP sequence (Figure 1K and 1L) a constant phase $\phi \approx 0$ was achieved over an off-resonance range of ±1 kHz. Beyond ±1 kHz range, all sequences (AHP, IAHP, and AHP + IAHP) show variations in amplitude and phase of magnetization components. Oscillations produced by the AHP were located between +1 and +5 kHz (Figure 1A-D), those produced by IAHP were located at negative offsets, between −5 and −1 kHz (Figure 1E-H), and the AHP + IAHP sequence showed oscillations at both positive and negative offsets between ±1 and ±5 kHz (Figure 1I-L), thereby corresponding to a reduced oscillation-free zone.

Three-dimensional (3D) plots of simulation results for AHP and AHP + IAHP show that the asymmetric/symmetric behavior of magnetization and phase and oscillations were maintained for any RF amplitude, while the oscillation-free zone increased linearly with the increased peak B_1 (Figure 2A-F). Whilst for AHP full excitation (M_z = 0) was achieved only on-resonance and was independent of the RF amplitude (Figure 2C), for AHP + IAHP an improved excitation was achieved over an offset range that increased linearly with RF amplitude (Figure 2D).

When comparing the AHP + IAHP pulse with the BIR-4 pulse[12] with an identical AHP segment, both disadvantages and advantages were observed (Figures 1 and 2): although the excitation bandwidth of AHP + IAHP sequence was slightly narrower than that of BIR-4 (Figures 1I, 1M, 2B, and 2G), the oscillation-free zone was comparable (i.e. narrower in both cases compared with the AHP pulse). In terms of saturation effects, a slightly improved off-resonance excitation (Figures 1J and 2D) was observed versus the BIR-4 pulse (Figures 1N and 2H). Furthermore, the AHP + IAHP pulse provided a symmetric and uniform phase relative to the carrier frequency (Figures 1K, 1L, and 2F), compared with the off-resonance asymmetric phase behavior noted for the BIR-4 pulse (Figures 1O, 1P, and 2I).

3.2 | In vitro ^{23}Na MRI

The in vitro ^{23}Na images obtained for AHP, IAHP, AHP + IAHP, and BIR-4 demonstrated a uniform excitation throughout the sensitive volume of the coil, as no absence of signal was observed in specific areas within the sensitive volume (Figure 3A-L). The pairs of magnitude and phase of images obtained using AHP (Figure 3A and 3C) or IAHP (Figure 3D and 3F) and AHP + IAHP (Figure 3G and 3I) sequences were asymmetric and symmetric relative to the carrier frequency (Figure 3B, 3E, and 3H), in agreement with Bloch simulations. Additionally, the off-resonance magnitudes of images obtained using the BIR-4 sequence (Figure 3J and 3L) were symmetric relative to the carrier frequency (Figure 3K), similarly to those obtained using the AHP + IAHP sequence, while the phases of images obtained with BIR-4 (Figure 3J-L) were rather similar to those obtained using the IAHP pulse (Figure 3D-F), in agreement with Bloch simulations. The symmetric/asymmetric behavior of image characteristics obtained using all sequences was further confirmed by the magnitude values on- and off-resonance of these images, although the BIR-4 pulse required higher voltage to achieve the adiabatic condition on-resonance.

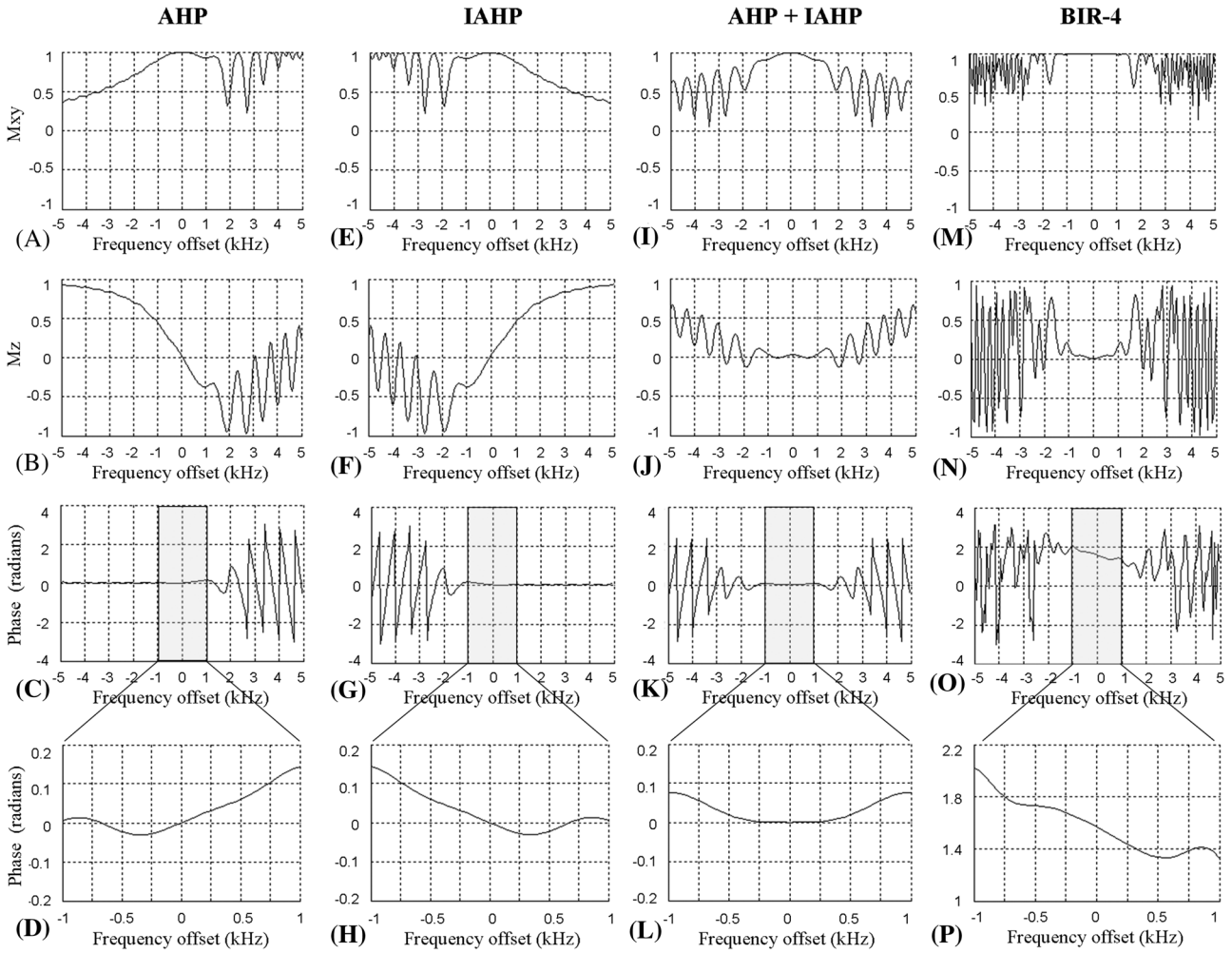

FIGURE 1 Bloch simulations for evaluating and comparing the performance of four adiabatic sequences (AHP, IAHP, AHP + IAHP, and BIR-4 with an identical AHP segment) as a function of frequency offsets using a fixed RF amplitude ($\gamma B_1/2\pi$) above the adiabaticity condition. Simulated magnetization and phase behavior of each sequence using $\gamma B_1/2\pi$ = 2 kHz over an offset range of ±5 kHz (±1 kHz for phase plots D, H, L, and P) relative to the carrier frequency. The AHP pulse (A-D) behaves as a mirror of the IAHP pulse (E-H) and both are asymmetric relative to the carrier frequency (A-H), whereas the AHP + IAHP pulse is symmetric relative to the carrier frequency (I-L). Although the AHP + IAHP sequence has a narrower excitation bandwidth (I) compared with BIR-4 using an identical AHP segment (M), an improved saturation (J) and symmetric phase response (K, L) was observed off-resonance compared with BIR-4 (N-P)

3.3 | In vitro ^{13}C MRS

The measured ^{13}C excitation bandwidth on formic acid using AHP + IAHP or BIR-4 sequences was found to be symmetric relative to the carrier frequency of the pulse (Figure 4C and 4D), while it was asymmetric using AHP or IAHP sequences (Figure 4A and 4B). Furthermore, the measured excitation bandwidth agreed well with the simulated transverse magnetization (M_{xy}) at the corresponding $\gamma B_1/2\pi$ for AHP (650 Hz), as shown in (Figure 4A-D).

The ^{13}C longitudinal relaxation time T_1 of glucose β measured using the inversion recovery method was 1.2 s. The signal intensities of the glucose β peaks off-resonance (±1 kHz) using a T_R of 1 s and 64 averages were asymmetric relative to the carrier frequency when using the AHP or IAHP sequence (Figure 4E and 4F), whereas they were symmetric when using the AHP + IAHP sequence (Figure 4G). Moreover, the ratio of the SNR off-resonance at −1 kHz and +1 kHz, i.e. SNR(−1 kHz)/SNR(+1 kHz), was approximately 2 for the AHP or IAHP sequence, whereas it was approximately 1.1 for the AHP + IAHP sequence, further demonstrating the symmetric excitation of metabolites off-resonance obtained with the AHP + IAHP sequence in contrast to the AHP or IAHP sequence. Furthermore, the signal intensities of glucose β peaks off-resonance (±1 kHz) were in agreement with the simulated averaged steady-state transverse magnetization (M_{xy}) response off-resonance for the AHP, IAHP, and AHP + IAHP sequences (Figure 4I-K). In particular, the sum of signal intensities at −1 kHz (Figure 4I and 4J, blue) is higher than at +1 kHz for the AHP or IAHP sequence (Figure 4I and 4 J, red), whereas these are comparable for the AHP + IAHP sequence (Figure 4K). By contrast, the

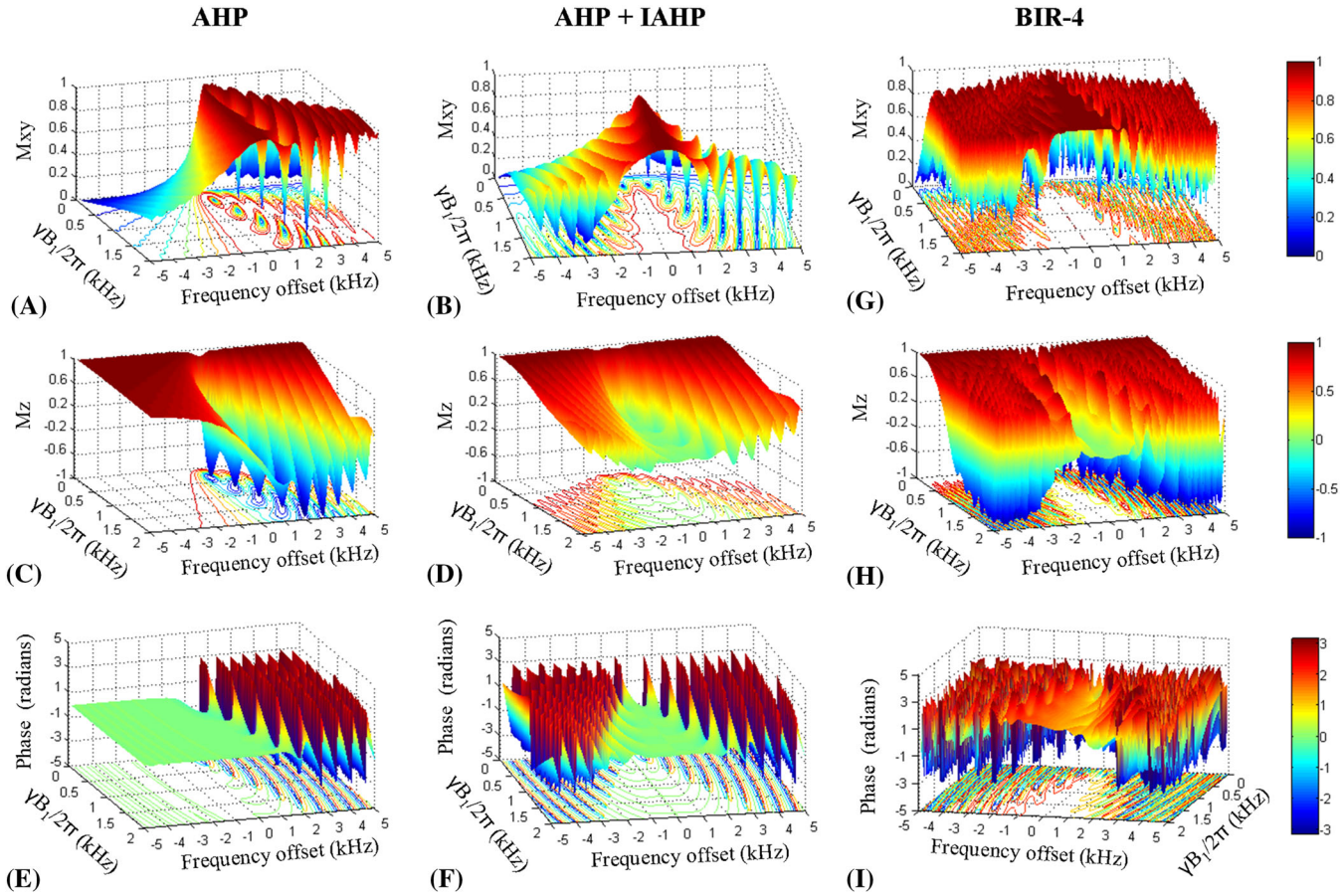

FIGURE 2 Bloch simulations for evaluation and comparison of the performance of three sequences (AHP, AHP + IAHP, and BIR-4) as a function of frequency offsets and RF amplitude ($\gamma B_1/2\pi$). The asymmetry of AHP (A, C, E) and the symmetry of AHP + IAHP (B, D, F) are maintained for any RF amplitude. Exact excitation occurs only on-resonance for AHP and is independent of the RF amplitude (C), whereas for AHP + IAHP an improved excitation is achieved over an offset range that increases linearly with RF amplitude (D), as for the BIR-4 pulse (H). In addition, the off-resonance phase behavior of the AHP + IAHP is symmetric and flat for any RF amplitude (F), in contrast to AHP (E) and BIR-4 (I)

signal intensities of glucose β peaks off-resonance (±1 kHz) obtained using the BIR-4 pulse were slightly asymmetric relative to the carrier frequency (Figure 4H), in slight disagreement with the simulated averaged steady-state transverse magnetization (M_{xy}) off-resonance (Figure 4L). Furthermore, the on-resonance signal intensity of glucose β obtained using the BIR-4 pulse was lower compared with that using AHP + IAHP, which in turn was lower than that using the AHP or IAHP pulses individually. In contrast, all sequences provided a similar on-resonance signal intensity of formic acid, although again the BIR-4 pulse required higher voltage to achieve the adiabatic condition.

3.4 | In vivo ^{13}C MRS

Spectra from in vivo non-localized ^{13}C MRS performed on the calf of a healthy male volunteer are shown with the same vertical scale in Figure 5A-D. The natural abundance glycogen C_1 resonance from the gastrocnemius muscle was detected in vivo at 100.5 ppm. In addition, triglyceride resonances attributed mainly to the subcutaneous adipose tissue (i.e. lipids) were detected in vivo, including glycerol C_2 and C_1, C_3 (62 ppm and 73 ppm), unsaturated CH_2 and saturated CH carbons of the aliphatic chain (30 ppm and 130 ppm), and the methyl carbon resonance (15 ppm). Zero and first order phase correction was applied to all measurements with identical parameters. In contrast to the spectrum obtained with the AHP or IAHP sequence, the spectrum obtained with the AHP + IAHP sequence was characterized by a flat baseline (Figure 5C). Consequently, intensities of the spectral lines at different offsets relative to the frequency of the pulse were close to those theoretically predicted when using the AHP, IAHP, or AHP + IAHP sequence. Similarly to the spectrum obtained with the AHP or IAHP pulse, the baseline of the spectrum obtained with the BIR-4 pulse was slightly distorted in a rather similar way to that using the IAHP sequence (Figure 5B and 5D), attributed to the similar phase dependence produced by both IAHP and BIR-4 pulses. Furthermore, the on-resonance signal intensity of glycogen C_1 measured with the BIR-4 pulse was lower compared with that obtained with the AHP + IAHP sequence, the latter also lower than that obtained with AHP or IAHP, in agreement with in vitro results for the glucose β phantom. In contrast, the BIR-4 pulse provided the highest lipid signals off-resonance.

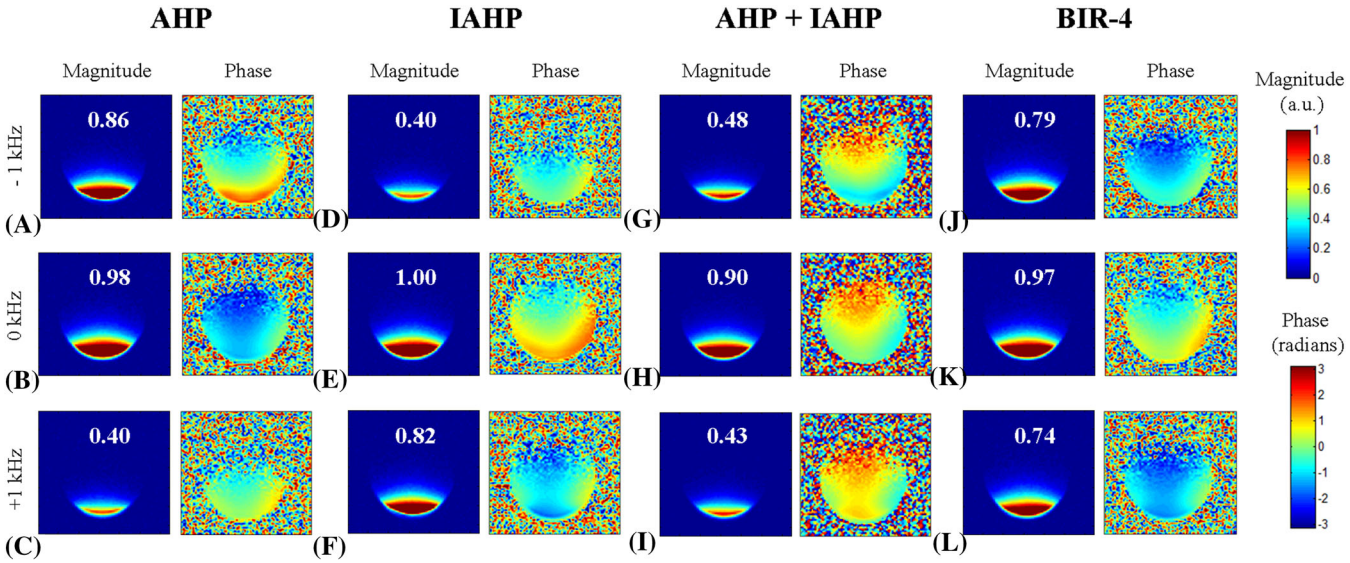

FIGURE 3 In vitro ^{23}Na images of 100 mM NaCl solution using a ^{23}Na-linear/^{1}H-quadrature surface coil. Images were obtained as transverse projections in the absence of slice gradient using a 2D FLASH sequence with adiabatic excitation. Both magnitude and phase are depicted for AHP (A-C), IAHP (D-F), AHP + IAHP (G-I), and BIR-4 (J-L). Images were acquired on-resonance (B, E, H, K) and offresonance at −1 kHz (A, D, G, J) and at +1 kHz (C, F, I, L). The numbers in the magnitude images are the normalized average magnitudes. (NMR protocol: FLASH 2D sequence using AHP, IAHP, or BIR-4 pulse for excitation (2 ms), T_R = 300 ms, T_E = 3.7 ms, FOV = 128 × 128 × 6 mm^3, matrix 64 × 64 × 1, slice thickness = 6 mm, spatial resolution = 2 × 2 × 6 mm^3, bandwidth = 260 Hz, 5 averages)

3.5 | In vivo ^{23}Na MRI

^{23}Na images obtained from the calf of a healthy male volunteer are shown in Figure 6. The pairs of magnitude and phase off-resonance for images obtained using AHP (Figure 6A and 6C) or IAHP (Figure 6D and 6F) and AHP + IAHP (Figure 6G and 6I) sequences were asymmetric and symmetric, respectively, relative to the carrier frequency (Figure 6B, 6E, and 6H), in agreement with Bloch simulations and with the ^{23}Na images in vitro. For images obtained using the BIR-4 pulse, the off-resonance magnitude (Figure 6J and 6L) was slightly asymmetric relative to the carrier frequency (Figure 6K), while the phases were rather similar to those obtained using the IAHP pulse (Figure 6D-F), in agreement with Bloch simulations and with ^{23}Na phases in vitro.

4 | DISCUSSION

This study evaluated the performance of a symmetric adiabatic excitation scheme based on the application of two AHP pulses with inverted phases in alternate scans[11,13] in humans at 7 T. The major advantage of this scheme over the single AHP excitation is a symmetric phase and excitation bandwidth relative to the carrier frequency, resulting in reduced baseline distortion and increasing the range of uniformity of ^{13}C peak intensities.

A symmetric phase behavior obtained by alternating the two AHP pulses was noted in the simulations, as well as symmetric transverse (M_{xy}) and longitudinal (M_z) magnetizations. Furthermore, simulations suggest that the resulting excitation bandwidth is proportional to the RF amplitude $\gamma B_1/2\pi$, for either the AHP or AHP + IAHP sequence. However, for the AHP pulse the full excitation (M_z = 0) was only achieved on-resonance and was independent of $\gamma B_1/2\pi$, whereas an improved excitation was achieved in a range of frequencies (proportional to $\gamma B_1/2\pi$) for AHP + IAHP (Figure 2C and 2D), similar to the behavior of the BIR-4 pulse. The inherent oscillations of the AHP + IAHP sequence on both sides off-resonance, compared with the AHP sequence in which there are oscillations only on one side, results in a reduced oscillation-free zone, which may be a disadvantage for the study of metabolites off-resonance beyond the effective excitation bandwidth. However, the reduced oscillation-free zone of AHP + IAHP is comparable to that of the BIR-4 pulse. In addition, the reduced pulse length of the AHP + IAHP sequence versus BIR-4 using an identical AHP segment results in a reduced specific absorption rate (SAR) when using the same T_R. Hence, both reduced pulse length and SAR suggests that the AHP + IAHP sequence could be advantageous in comparison with BIR-4 for MR applications in humans at very high field requiring short T_R, e.g. for temporal resolution in functional measurements or for an increase in the number of averages in the same time for low sensitivity nuclei with short relaxation time such as glycogen.

In vitro ^{23}Na MRI measurements using AHP, IAHP, AHP + IAHP, and BIR-4 pulses were in agreement with simulations in terms of asymmetry/symmetry, as suggested by the pairs of magnitudes at two equidistant offset resonances relative to the center frequency (Figure 3).

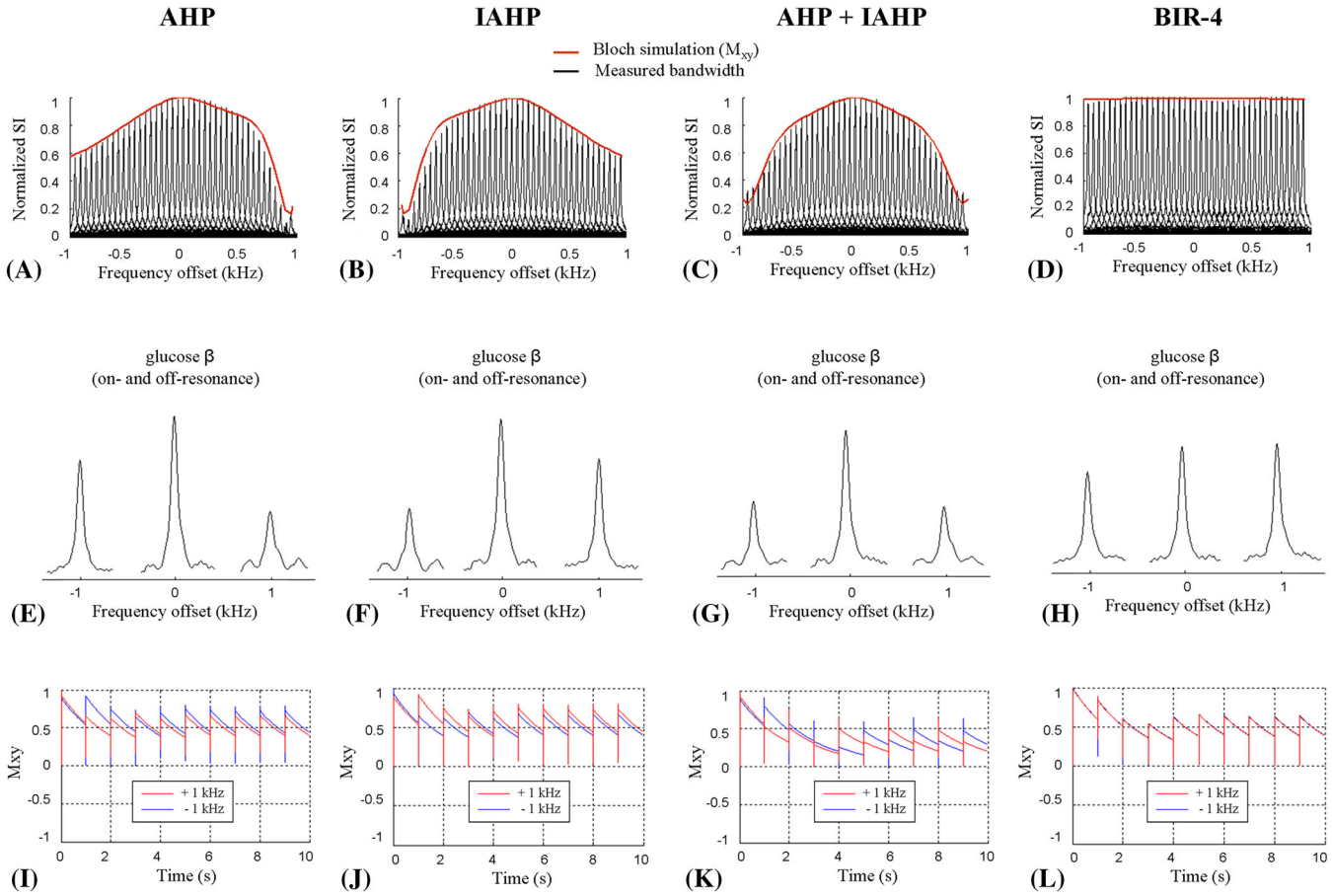

FIGURE 4 A-D, in vitro proton-decoupled ^{13}C NMR spectra with 99% ^{13}C-enriched formic acid using the AHP pulse (A), IAHP pulse (B), alternating AHP and IAHP pulses (C), and BIR-4 pulse (D). The bandwidth of each sequence was measured by exciting formic acid at frequency offsets in a range of ±1 kHz in 50 Hz steps (T_R = 10 s, vector size 2048, bandwidth 20 kHz, decoupling duration 87 ms, 2 averages). The simulated transverse magnetization (M_{xy}) is in very close agreement with the measured ^{13}C excitation bandwidth of formic acid using either AHP (A), IAHP (B), AHP + IAHP (C), or BIR-4 (D). E-H, in vitro proton-decoupled ^{13}C NMR spectra with glucose β using the AHP pulse (E), IAHP pulse (F), alternating AHP and IAHP pulses (G), and BIR-4 pulse (H). Spectra of glucose β are shown with the same vertical scale. I-L, Bloch simulations showing the averaged steady-state transverse magnetization (M_{xy}) response of AHP (I), IAHP (J), AHP + IAHP (K), and BIR-4 (L) for two frequency offsets, i.e. −1 kHz and +1 kHz. The transverse magnetization (M_{xy}) was simulated off-resonance following 10 excitations for 2 ms AHP or BIR-4 pulse, T_1 = 1.5 s, T_2 = 0.2 s, and T_R = 1 s. The effective signal intensities for AHP (I) are asymmetric off-resonance, i.e. the sum of signal intensities following 10 excitations for AHP at −1 kHz is higher than at +1 kHz, and vice versa for IAHP (J). In contrast, the effective signal intensities for AHP + IAHP and BIR-4 (K, L) sequences are symmetric off-resonance, i.e. the sum of signal intensities at −1 kHz is equivalent to that at +1 kHz

The very close agreement with Bloch simulations was enabled by using a T_R longer than the T_1 of sodium in solution (T_R > 5 T_1, T_1 ~ 50 ms) to ensure that magnetization was fully relaxed previous to each scan. In fact, the small asymmetry of the pairs of magnitudes off-resonance of ^{23}Na images obtained in the human calf using the BIR-4 pulse was attributed to possible differences in the required voltage on- and off-resonance in vivo and to the phase effect within a B_1 varying with the distance from the coil, rather than due to relaxation properties.

In vitro ^{13}C MRS measurements of fully relaxed formic acid were in excellent agreement with simulations in terms of symmetry and $\gamma B_1/2\pi$, as supported by the measured ^{13}C excitation bandwidth, which matches the simulated transverse magnetization (M_{xy}) (Figure 4A-D). The excellent agreement between the measurement and simulation was enabled by ensuring that the measured sample of formic acid was placed in a small glass sphere in the center of the ^{13}C coil, where the B_1 field was reasonably homogeneous. By comparing the effective excitation bandwidth obtained with AHP + IAHP pulses versus that obtained with AHP (or IAHP), although the AHP (or IAHP) pulse could lead to better results at +1 kHz (or −1 kHz) compared with AHP + IAHP, the asymmetric excitation obtained with AHP (or IAHP) relative to the carrier frequency would make it unsuitable for the evaluation of saturation factors of a range of different metabolites, such as in in vivo ^{13}C MRS using multiple averages and short T_R.

In vitro ^{13}C MRS measurements of T_1 weighted glucose β signal using the AHP, IAHP, or AHP + IAHP sequence were in agreement with the simulations in terms of asymmetry/symmetry, as supported by the glucose β signal intensities measured off-resonance while using short T_R (< 5T_1) (Figure 4E-G) and the simulated steady-state transverse magnetization (M_{xy}) off-resonance following 10 excitations with T_R = 1 s (Figure 4I-K). Although in vitro ^{13}C MRS measurements of T_1 weighted signal intensities off-resonance were performed using a single metabolite (glucose β),

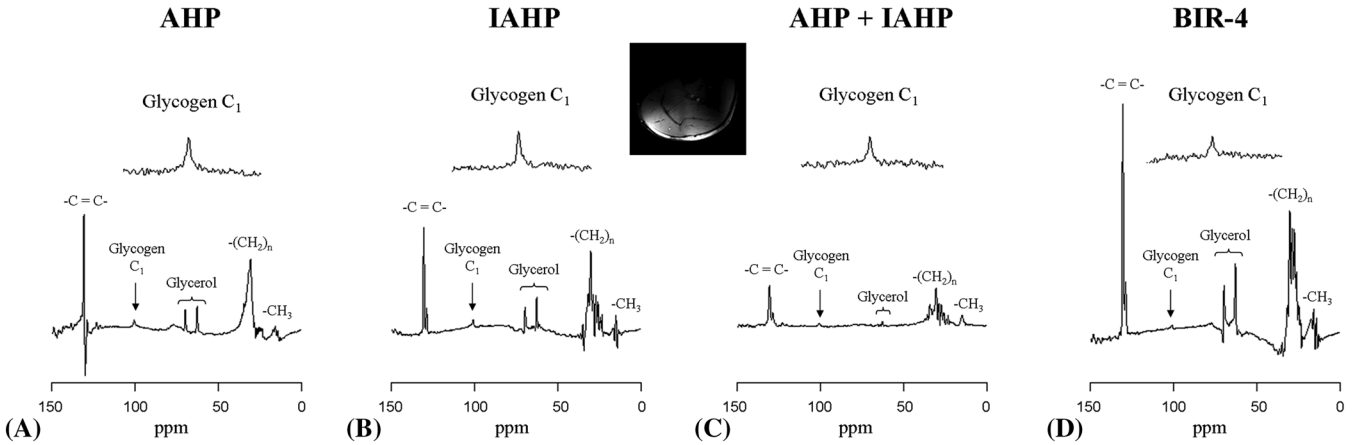

FIGURE 5 In vivo non-localized ^{13}C NMR spectra of the calf muscle from a male subject acquired in 4 min 15 s, 2 ms pulse acquire with adiabatic excitation using the AHP (A), IAHP (B), alternating AHP and IAHP (C), and BIR-4 pulses (D), 20 ms WALTZ-16 decoupling, T_R = 1.2 s, bandwidth = 20 kHz, 300 scans, vector size = 2048, zero filling = 2048, Gaussian function ($\exp[-t^2/2(0.02)^2]$) applied to the FID prior to Fourier transform. Spectra show detection of the glycogen C_1 resonance (100.5 ppm), glycerol moiety (62 ppm and 73 ppm), CH_2 and CH carbons of the aliphatic chain (30 ppm and 130 ppm), and methyl peak (15 ppm). All spectra are shown with the same vertical scale. Although zero and second order phase correction was applied to all measurements with identical parameters, the spectrum obtained with the AHP, IAHP, and BIR-4 sequences have a distorted baseline (A, B, D), whereas the spectrum obtained with the AHP + IAHP sequence is characterized by a flat baseline (C)

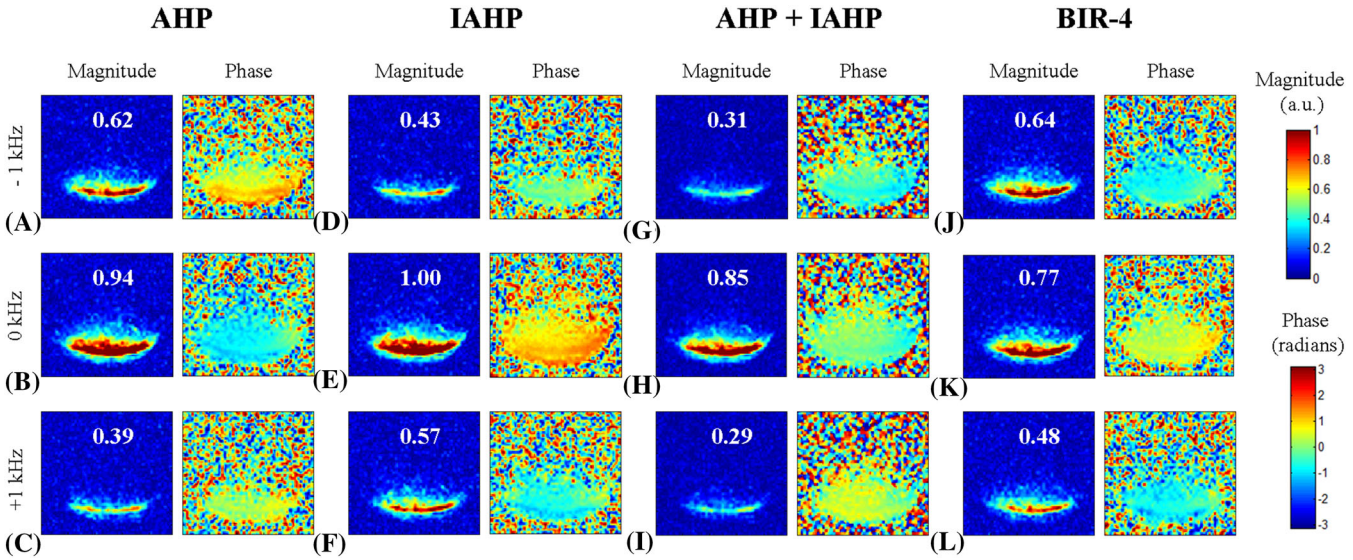

FIGURE 6 In vivo ^{23}Na images of the calf muscle from a male subject using a ^{23}Na-linear/^{1}H-quadrature surface coil. Images were obtained as transverse projections in the absence of slice gradient using a 2D FLASH sequence with adiabatic excitation. Both magnitude and phase are depicted for AHP (A-C), IAHP (D-F), AHP+IAHP (G-I), and BIR-4 (J-L). Images were acquired on-resonance (B, E, H, K) and off-resonance at −1 kHz (A, D, G, J) and at +1 kHz (C, F, I, L). The numbers in the magnitude images are the normalized average magnitudes. (NMR protocol: FLASH 2D sequence using AHP, IAHP, or BIR-4 pulse (2 ms) for excitation, T_R = 300 ms, T_E = 3.7 ms, FOV = 128 × 128 × 6 mm^3, matrix 64 × 64 × 1, slice thickness = 6 mm, spatial resolution = 2 × 2 × 6 mm^3, bandwidth = 260 Hz, 5 averages)

the symmetry of T_1 weighting with the carrier frequency is expected to hold in a spectrum including a variety of metabolites (i.e. in vivo ^{13}C spectra of human muscle or brain), even when the T_R is shorter than or comparable to the T_1 of the observed nucleus. The symmetric signal intensities obtained with the AHP + IAHP sequence suggest that T_1 weighting is symmetric with offset when using the AHP + IAHP sequence with a T_R shorter than (or equal to) the faster-relaxing resonance ($T_R \leq T_1$). In contrast, in vitro ^{13}C MRS measurements of the partially saturated (T_1 weighted) glucose β signal using the BIR-4 pulse resulted in a small disagreement with simulations in terms of symmetry, demonstrated by the glucose β signal intensities measured off-resonance while using short T_R (< $5T_1$) (Figure 4H) and the simulated steady-state transverse magnetization (M_{xy}) off-resonance following 10 excitations with T_R = 1 s (Figure 4L). This was attributed to the asymmetric phase off-resonance of the BIR-4 pulse and to the fact that the simulation was performed using a spatially homogeneous B_1. In fact, the signal intensities of formic acid peaks

off-resonance (±1 kHz) were in agreement in terms of asymmetry/symmetry with the simulated averaged steady-state transverse magnetization (M_{xy}) response off-resonance for all sequences, including BIR-4 (Figure 4A-D and 4I-L), due to the homogeneous B_1 field of the formic acid sample. Concerning the signal intensities of partially saturated glucose β on-resonance, a lower value using the AHP + IAHP sequence versus the AHP or IAHP pulse was observed, and this could be explained by the effect of inverting the phases within a B_1 varying with the distance from the coil. Similarly, the lower signal intensity of partially saturated glucose β on-resonance using the BIR-4 pulse was also attributed to the phase effect of the BIR-4 pulse in a B_1 varying with the distance from the coil (i.e. B_1 in the glucose β phantom). Effectively, the signal intensity of the formic acid peak on-resonance was similar for all sequences, in agreement with simulations.

The feasibility of the sequence was demonstrated on in vivo ^{13}C MR spectra of human calf. In particular, in vivo ^{13}C MRS measurements using either the AHP, IAHP, or AHP + IAHP sequence were in agreement with simulations as evidenced from the ^{13}C signal intensities off-resonance and baseline (Figure 5). While the baseline of the AHP and IAHP sequences appears distorted (in opposite directions), the baseline of the AHP + IAHP sequence became more flat. This suggests that the offset dependence of the phase inherent to the AHP or IAHP sequence could be alleviated by using the AHP + IAHP sequence, yielding both uniform flip angle and phase over the effective excitation bandwidth for any RF amplitude ($\gamma B_1/2\pi$). Although some distortions remained beyond the effective excitation bandwidth while using either the AHP or AHP + IAHP sequence (Figure 2A and 2B), this may be useful for selective peak suppression, as suggested previously.[19]

Despite the improved off-resonance phase behavior using the AHP + IAHP sequence, there is a loss in signal intensity in vivo, similar to that observed in the in vitro results of partially saturated glucose β, which may be due to the effect of inverting the phases in a B_1 varying with the distance from the coil across the sample (such as the B_1 in the glucose β phantom and in the muscle), independently of the T_R. As ^{13}C MRS measurements were made using multiple averaging, the potential presence of macroscopic motion (such as subject motion) may induce spin-phase variations from scan to scan, which could lead to signal loss. In particular, schemes that add/subtract in alternate scans, such as the AHP + IAHP sequence, may be more susceptible to losing signal due to motion—although this could be alleviated by the use of motion correction. In contrast, diffusion of spins could lead to signal loss due to the spin-phase dispersal across the sample. In this context, metabolites with fast diffusion of spins may be more susceptible to lose signal upon inverting the pulse phase for a given pulse length—but this is not expected to be observed in the case of molecules with slow diffusion of spins such as glycogen.

Although the proposed sequence has been evaluated for ^{13}C MRS and ^{23}Na MRI, it can be used for any other nucleus.

We conclude that it is feasible to apply two AHP pulses with inverted phases in alternate scans to induce symmetric excitation and constant phase in the ^{13}C NMR spectrum and in the ^{23}Na NMR images at 7 T. In addition, the presented approach provides symmetric offset dependence of T_1 weighted signal intensities, suggesting possible extension of this technique for ^{13}C MRS and ^{23}Na MRI measurements in human brain.

ACKNOWLEDGEMENTS

This research was supported in part by the Centre d'Imagerie Biomédicale (CIBM) of the Université de Lausanne (UNIL), Université de Genève (UNIGE), Hôpitaux Universitaires de Genève (HUG), Centre Hospitalier Universitaire Vaudois (CHUV), Ecole Polytechnique Fédérale de Lausanne (EPFL), and Leenaards and Jeantet Foundations. The authors would like to thank Dr Bernard Lanz for insightful discussions.

ORCID

Eulalia Serés Roig https://orcid.org/0000-0002-6524-3826

REFERENCES

1. Beckmann N. *Carbon-13 NMR Spectroscopy in Biological Systems*. San Diego, California: Academic; 1995.
2. Rothman DL, De Feyter HM, de Graaf RA, Mason GF, Behar KL. ^{13}C MRS studies of neuroenergetics and neurotransmitter cycling in humans. *NMR Biomed*. 2011;24(8):943-957.
3. Hoult DI, Richards RE. The signal-to-ratio of the nuclear magnetic resonance experiment. *J Magn Reson*. 1976;24(1):71-85.
4. Slichter CP. *Principles of Magnetic Resonance*. 2nd ed. Berlin, Germany: Springer; 1979:24.
5. Garwood M, Ugurbil K. B_1 insensitive adiabatic RF pulses. In: Diehl P, Fluck E, Gunther H, Kosfeld R, Seelig J, eds. *NMR Basic Principles and Progress*. Vol.27 Berlin, Germany: Springer; 1992:109-147.
6. Tannus A, Garwood M. Adiabatic pulses. *NMR Biomed*. 1997;10(8):423-434.
7. de Graaf RA, Nicolay K. Adiabatic RF pulses: applications to in vivo NMR. *Concepts Magn Reson*. 1997;9:247-268.
8. Garwood M, DelaBarre L. The return of the frequency sweep: designing adiabatic pulses for contemporary NMR. *J Magn Reson*. 2001;153:155-177.
9. Silver MS, Joseph RI, Hoult DI. Highly selective π/2 and π pulse generation. *J Magn Reson*. 1984;59:347-351.
10. Bendall MR, Pegg DT. Uniform sample excitation with surface coils for in vivo spectroscopy by adiabatic rapid half passage. *J Magn Reson*. 1986;67:376-381.
11. Gruetter R, Boesch C, Martin E, Wüthrich K. A method for rapid evaluation of saturation factors in in vivo surface coil NMR spectroscopy using B_1-insensitive pulse cycles. *NMR Biomed*. 1990;3(6):265-271.

12. Garwood M, Ke Y. Symmetric pulses to induce arbitrary flip angles with compensation for RF inhomogeneity and resonance offsets. *J Magn Reson*. 1991;94:511-525.
13. El-Sharkawy AM, Schär M, Ouwerkerk R, Weiss RG, Bottomley PA. Quantitative cardiac ^{31}P spectroscopy at 3T using adiabatic pulses. *Magn Reson Med*. 2009;61:785-795.
14. Adriany G, Gruetter R. A half-volume coil for efficient proton decoupling in humans at 4 tesla. *J Magn Reson*. 1997;125:178-184.
15. Shaka AJ, Keeler J, Frenkiel T, Freeman R. An improved sequence for broadband decoupling: WALTZ-16. *J Magn Reson*. 1983;52:335-338.
16. Gruetter R, Adriany G, Choi IY, Henry PG, Lei H, Oz G. Localized in vivo ^{13}C NMR spectroscopy of the brain. *NMR Biomed*. 2003;16:313-338.
17. Bax A. A simple method for the calibration of the decoupler radiofrequency field strength. *J Magn Reson*. 1983;52:76-80.
18. Gruetter R, Tkac I. Field mapping without reference scan using asymmetric echo-planar techniques. *Magn Reson Med*. 2000;43:319-323.
19. Bansal N. Off-resonance performance of adiabatic excitation pulses and their use for selective peak suppression. *J Magn Reson B*. 1993;102:73-76.

How to cite this article: Serés Roig E, Xin L, Gallichan D, Mlynarik V, Gruetter R. Improved off-resonance phase behavior using a phase-inverted adiabatic half-passage pulse for ^{13}C MRS in humans at 7 T. *NMR in Biomedicine*. 2019;32:e4171. https://doi.org/10.1002/nbm.4171